

## Effect of spiral reinforcement on flexural-shear-torsional seismic behavior of reinforced concrete circular bridge columns

Abdeldjelil Belarbi<sup>†</sup>, Suriya Prakash<sup>‡</sup> and Young-Min You<sup>‡†</sup>

*Department of Civil, Environmental and Architectural Engineering,  
Missouri University of Science and Technology, Rolla, Missouri, USA*

*(Received July 30, 2008, Accepted July 15, 2009)*

**Abstract.** This paper investigates the behavior of reinforced concrete (RC) circular columns under combined loading including torsion. The main variables considered in this study are the ratio of torsional moment to bending moment (T/M) and the level of detailing for moderate and high seismicity (low and high transverse reinforcement/spiral ratio). This paper presents the results of tests on seven columns subjected to cyclic bending and shear, cyclic torsion, and various levels of combined cyclic bending, shear, and torsion. Columns under combined loading were tested at T/M ratios of 0.2 and 0.4. These columns were reinforced with two spiral reinforcement ratios of 0.73% and 1.32%. Similarly, the columns subjected to pure torsion were tested with two spiral reinforcement ratios of 0.73% and 1.32%. This study examined the significance of proper detailing, and spiral reinforcement ratio and its effect on the torsional resistance under combined loading. The test results demonstrate that both the flexural and torsional capacities are decreased due to the effect of combined loading. Furthermore, they show a significant change in the failure mode and deformation characteristics depending on the spiral reinforcement ratio. The increase in spiral reinforcement ratio also led to significant improvement in strength and ductility.

**Keywords:** circular columns; combined loadings; confinement; ductility; flexure; interaction diagrams; shear; spiral reinforcement ratio; torsion.

---

### 1. Introduction

Combined loading including torsion, axial, shear, and flexure occur in reinforced concrete (RC) members such as arch ribs, L shaped bridge piers, spiral stair cases, bridges with outrigger bents, and spandrel beams. The loading can be as simple as gravity or as challenging as that resulting from seismic excitations. Previous research has focused on the overall behavior and ultimate strength of RC members subjected to various combinations of transverse shear force, axial force, and bending moment. However, studies examining the behavior of members under combined loading including torsion have been limited. Reinforced concrete bridge columns with irregular three-dimensional bridge configurations could result in significant torsional moments in addition to axial, flexure, and

---

<sup>†</sup> Distinguished Professor, Corresponding author, E-mail: [belarbi@mst.edu](mailto:belarbi@mst.edu)

<sup>‡</sup> Ph.D., Candidate, E-mail: [spsg33@mst.edu](mailto:spsg33@mst.edu)

<sup>‡†</sup> Post Doctoral Fellow, E-mail: [youngmin@mst.edu](mailto:youngmin@mst.edu)

shear forces during earthquake events. The addition of torsion is more likely in skewed or horizontally curved bridges, bridges with unequal spans or column heights, and bridges with outrigger bents. Construction of bridges with these configurations is often unavoidable due to site constraints. In addition, multidirectional earthquake motions (including significant vertical motions), structural constraints due to a stiff decking, movement of joints, abutment restraints, and soil conditions may also lead to combined loading effects. This combination of seismic loading and structural constraints can result in complex flexural and shear failure of bridge columns. Rational models are available to analyze the interaction between axial compression and flexure. A number of researchers have investigated extensively the behavior of columns under flexure and shear with and without axial compression. Park and Ang (1985), Priestly and Benzoni (1996), Priestly *et al.* (1998), Lehman *et al.* (1998), Elwood and Moehle (2005), and Mostafaei and Kabeyasawa (2007), have proposed various models for predicting seismic performance of column members under flexure-shear loads.

The presence of torsion along with shear and flexure increases the possibility of shear failure, and the understanding of the interaction among flexure, shear, and torsion in the behavior of RC bridge columns is limited. Very few experimental results have been reported on the behavior of RC columns under combined loading (Otsuka *et al.* 2004, Tirasit and Kawashima 2007, 2008, Belarbi *et al.* 2008a, 2008b, Suriya Prakash *et al.* 2008). Although a few studies have been carried out on the behavior of circular columns under combined loading, the behavior is not fully understood owing to many parameters that affect the behavior under combined loading. Hsu and Wang (2000) studied the performance of composite columns with H-steel sections under combined loading. They found that the flexural capacity and ductility of composite columns decreased when a constant torsion was applied simultaneously with flexure and axial load. Otsuka *et al.* (2004) tested nine rectangular columns under pure torsion, bending/shear, and various ratios of combined flexure and torsion. They concluded that the pitch of the hoop lateral tie significantly affects the hysteresis loop of torsion. Later, Tirasit and Kawashima (2007) reported tests on RC columns under various levels of rotation-to-drift ratios. They reported that the flexural capacity of RC columns decreases as the rotation-to-drift ratio increases, and damage tends to occur above the flexural plastic hinge region.

Belarbi *et al.* (2008a) have discussed the state of current research on behavior of RC columns under combined loading and the scope of further research. They carried out seismic analyses of bridge models for a practical range of earthquake motions. The results from their study clearly showed that the bridge columns in the bents closest to the bridge abutments were subjected to significantly higher torsion-to-bending moment (T/M) ratios of between 0.33 and 0.52 compared to the bents closest to the center of the bridge. They also concluded that the softening of concrete strength in the presence of shear and torsion and confinement of concrete due to transverse reinforcement play a major role in determining the ultimate strength of concrete sections under combined loading. They suggested that simplified constitutive models should be developed to incorporate softening and confinement effects. Belarbi *et al.* (2008b) tested several circular columns under combined loading at various T/M ratios. They reported that a spiral reinforcement ratio which might be adequate from the flexural design point of view may not be adequate in the presence of torsional moments. They observed that the effects of combined loading reduce flexural and torsional capacities and affect failure modes and deformation characteristics. They found that with an increase in T/M ratios, the energy dissipation capacity decreases. Recently, the damage based design approach was also proposed for RC columns under combined loading including torsion (Suriya Prakash and Belarbi 2009).

A review of previously published studies indicates that very few investigations have been carried

out on the behavior of RC columns under combined loading. In current literature, only limited information is available on the effect of increasing the transverse reinforcement ratio on the behavior of RC columns under combined loading. This paper presents the results of experimental and finite element studies on the performance of RC circular columns subjected to a cyclically combined loading with two levels of spiral reinforcement ratios. The experimental and analytical results of this study will provide the basis for further development of interaction surfaces and design guidelines for circular RC columns subjected to combined loading including torsion. Moreover, this paper presents the results of tests on seven columns: one under cyclic flexure-shear, two under pure cyclic torsion, and four under combined cyclic flexure-shear and torsion. It compares the hysteretic lateral load-displacement, torsional moment-twist response, reinforcement strain variations, and damage characteristics.

## 2. Experimental program

### 2.1 Specimen details

Half-scale column specimens were designed to be representative of typical existing bridge columns. The specimen dimensions and reinforcement layout are shown in Fig. 1. Each circular RC column

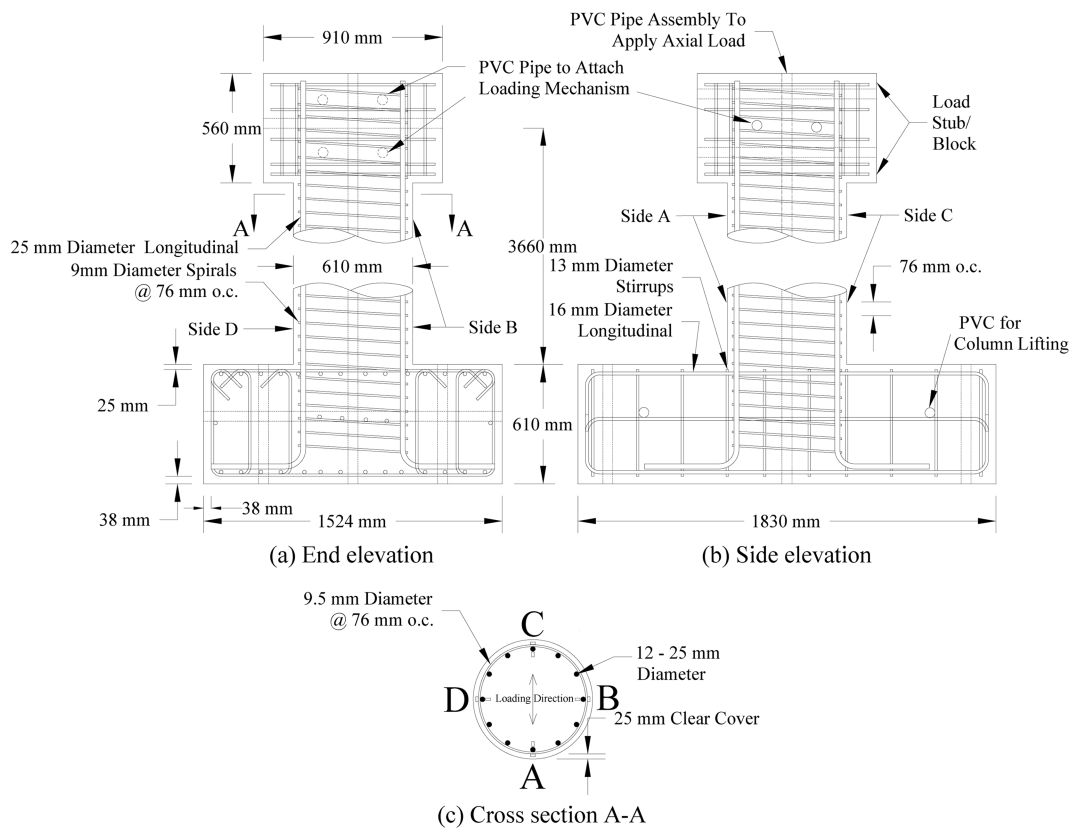


Fig. 1 Column and footing sectional details

specimen had a diameter (D) of 610 mm. and a clear concrete cover of 25 mm. These specimens were fabricated in the High Bay Structures Laboratory at Missouri University of Science and Technology (Missouri S&T). The total height of the columns was 3.8 m, with an effective height (H) from the top of the footing to the centerline of the applied forces of 3.66 m. Typically, axial load due to superstructure dead weight transferred to the bridge columns varies between 5 and 10% of the capacity of the columns. Hence, this study assumed an axial load of 7% of the concrete compression capacity of the columns. Twelve 25 mm- diameter bars were used as longitudinal reinforcement. The longitudinal reinforcement ratio was 2.1% for all columns tested. To study the effectiveness of increasing the spiral reinforcement ratio, columns under combined loading were tested under T/M ratios of 0.2 and 0.4 with spiral reinforcement ratios of 0.73% and 1.32%, respectively.

## 2.2 Material properties

The concrete was supplied by a local ready mix plant. It had requested 28-day cylinder strength of 34 MPa. Standard tests were conducted for compressive strength, splitting tensile strength, modulus of rupture of concrete, and tension tests on steel coupons. The actual material properties of the concrete and steel reinforcement as measured on the day of testing of the column specimen are given in Table 1.

## 2.3 Test set-up and instrumentation

Reversed cyclic bending and shear, pure torsion, and combined bending, shear, and torsion were generated by controlling two horizontal servo-controlled hydraulic actuators shown schematically in Fig. 2. Cyclic bending and shear was created by applying equal forces with the two actuators. Pure torsion was created by applying equal but opposite forces with the two actuators. Combined cyclic torsion, shear and bending were imposed by applying different forces or displacements with each

Table 1 Mechanical properties of concrete and steel used in test columns

Properties	Test Columns						
	H/D(6) T/M(0)	H/D(6) T/M( $\infty$ )	H/D(3) T/M( $\infty$ )	H/D(6) T/M(0.4)	H/D(6) T/M(0.2)	H/D(6) T/M(0.4)	H/D(6) T/M(0.2)
Compressive Strength ( $f'_c$ , MPa)	33.4	37.9	28.0	25.7	26.5	41.2	41.2
Modulus of Rupture ( $f_{cr}$ , MPa)	3.52	3.86	3.25	3.52	3.38	3.93	3.86
Splitting Tensile Strength ( $f_t$ , MPa)	3.44	3.56	2.41	3.44	2.48	2.81	2.62
Spiral Reinforcement Ratio (%)	0.73	0.73	1.32	0.73	0.73	1.32	1.32
Spiral Yield Strength ( $f_{ly}$ , MPa)	450						
Longitudinal Yield Strength ( $f_{ly}$ , MPa)	457						

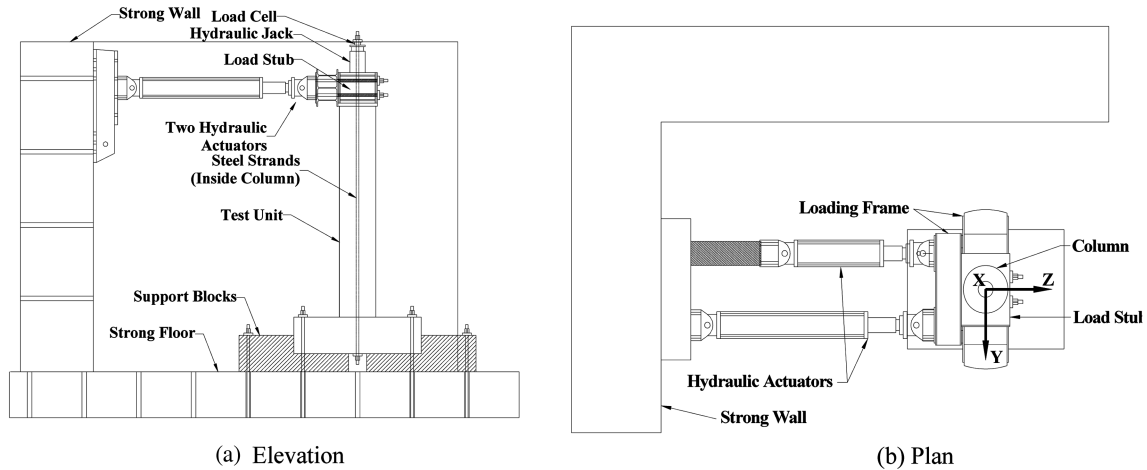


Fig. 2 Test and loading setup

actuator. The ratio of applied bending moment to torsional moment was controlled by maintaining the ratio of the forces in the two actuators.

A hydraulic jack on top of the column was used to apply the axial load. The jack transferred the load to the column via seven unbonded high-strength prestressing steel strands running through a duct in the center of the column and anchored to a plate beneath the test specimen. A target 7% axial load ratio was applied to simulate the dead load on a bridge column. The unbonded external prestressing in a structural system should be treated as an internal indeterminate system for an accurate analysis which is different from the assumption of uniform compression stresses on column when the loads are applied through a hydraulic jack. However, broader and thicker steel plates were used for distribution of loads from the jack to the loading block. Similarly, a thicker and broader steel plate was used for load distribution beneath the foundation. This resulted in more uniform distribution of compression load in the test portion of column member (i.e., from top of foundation to the center of the loading block). Moreover, the strands were going through a duct which is closer to the flexural neutral axis. In torsion, the outer portion of concrete column is the most effective in resisting torsion and the strands for prestressing will not influence the behavior as such. Hence, the structural differences between using unbonded prestressing strands and hydraulic jack in terms of overall behavior will not be significantly affected, except that with the use of internal prestressing tendons, the P-delta effect is eliminated for analysis simplicity.

The columns were heavily instrumented to measure the applied loads, deformation, and internal strain. Load cells in the horizontal hydraulic actuators measured the applied forces. The axial load in the steel strands was measured using a load cell placed between the hydraulic jack and the top of the load stub. The twist and horizontal displacement of the columns were measured using string transducers at multiple heights above the column footing. Electric strain gages on the longitudinal and transverse reinforcement were used to measure the strains in the bars in sides A, B, C, and D (See Fig. 3). The typical string transducer and strain gage locations for the columns tested under bending-shear, combined bending, shear and torsion and pure torsion along the height of the column are shown in Fig. 3.

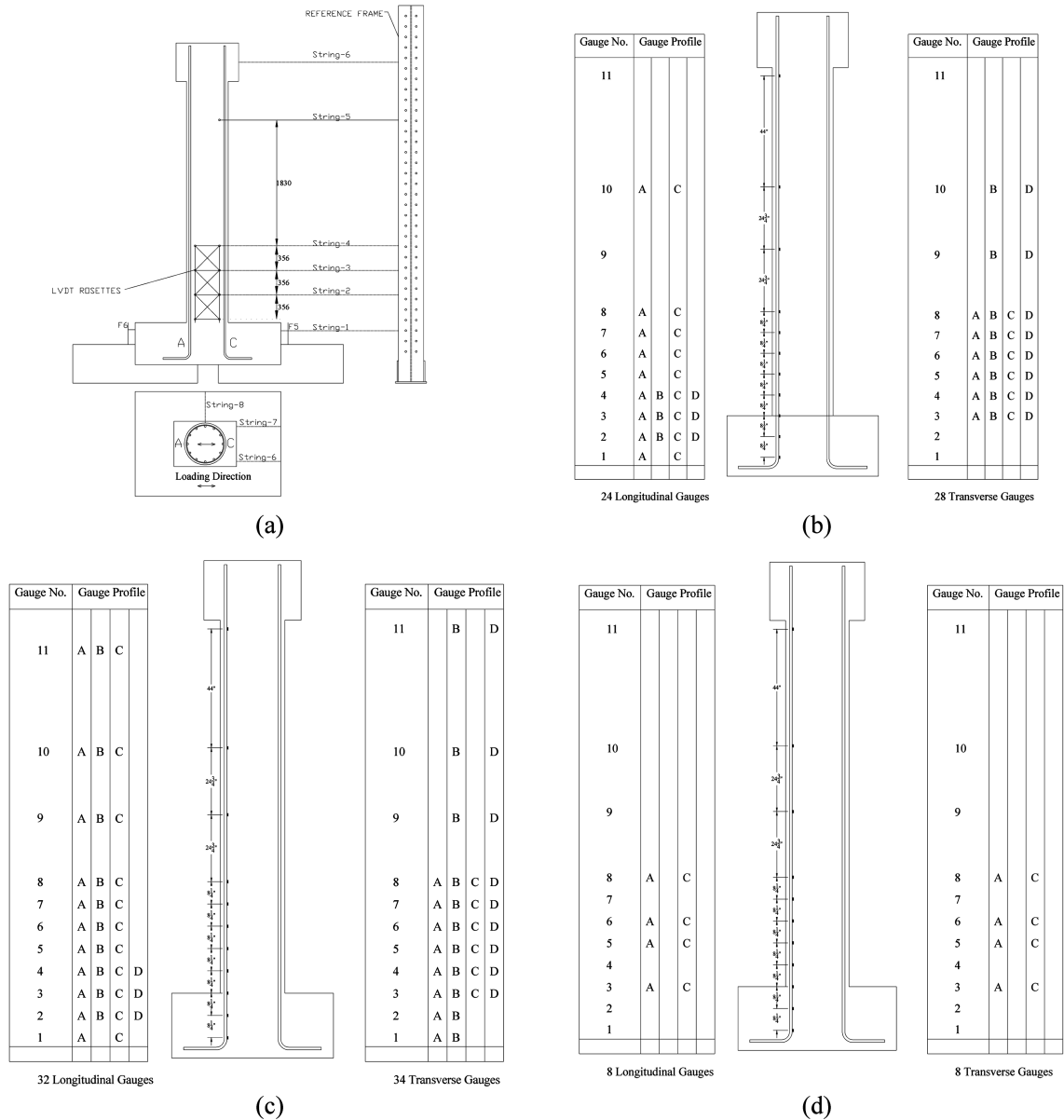


Fig. 3 Instrumentation for test column (a) location of string transducers and LVDT rosettes, (b) Strain gage locations for bending shear (c) Strain gage locations for combined bending, shear and torsion and (d) Strain gage locations for pure torsion

### 2.4 Loading protocol

Columns tested under bending and shear and combined bending, shear and torsion were conducted in load control mode until first yielding of the longitudinal bars. The load was applied in load control mode at intervals of 25%, 50%, 75%, and 100% of the predicted yielding force, corresponding to the yielding of the first longitudinal bar ( $F_y$ ). The horizontal displacement corresponding to

yielding of the first longitudinal bar was defined as displacement ductility ( $\mu_{\Delta}$ ) of 1.0. The column under pure torsion was loaded under load control at intervals of 25%, 50%, 75%, and 100% of the estimated yielding of the first spiral ( $T_y$ ). The rotation corresponding to yielding torque, which in turn corresponded to the first yielding of spiral reinforcement, was defined as a rotational ductility ( $\mu_{\theta}$ ) of 1.0. After the first yield, tests were continued in displacement control at specified levels of ductility and with T/M ratio controlled at desired levels up to failure of the specimens. Three loading cycles were performed at each ductility level. The three cycles were intended to assess the degradation of column strength and stiffness. The loading were applied along the direction A-C following the sign convention shown in Fig. 1. The loading along directions A-C and C-A were defined as positive (unlocking of spiral) and negative (locking of spiral) cycles, respectively.

### 3. Test results and discussions

#### 3.1 Column under bending and shear

After cyclical loading to 50% of  $F_y$ , the column tested under bending and shear exhibited flexural cracks near the bottom on sides A and C (Fig. 1). With higher levels of loading, these cracks continued to grow and new cracks appeared on both sides of the column. The concrete cover started spalling at a drift of about 3.2% (at a displacement of 117 mm). Application of symmetric loading at ductility levels higher than 8.0 were not possible because of the actuator stroke limitation. Spacers were attached between the actuators and the column, and the displacement was applied only in the A-C direction after ductility 8.0. Failure of the specimen began with the formation of a flexural plastic hinge at the base of the column, followed by core degradation and finally by the buckling of longitudinal bars on the compression side at a displacement of 460 mm (at a ductility of

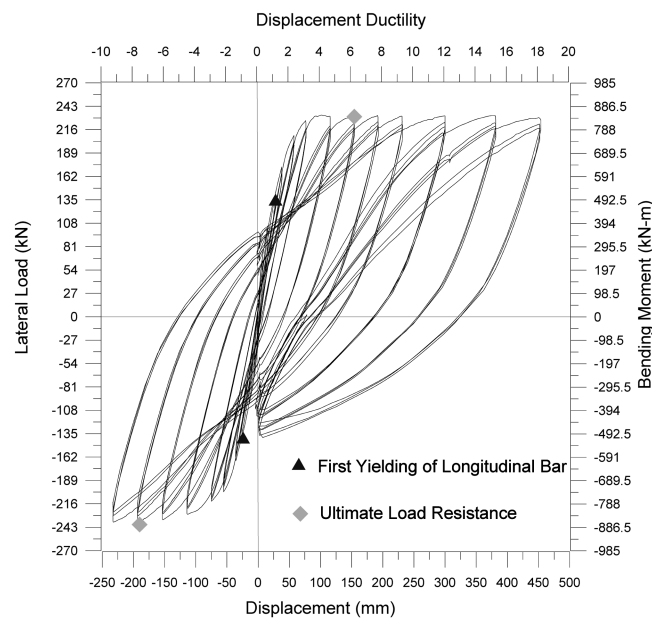


Fig. 4 Flexural hysteresis curves of column under bending shear

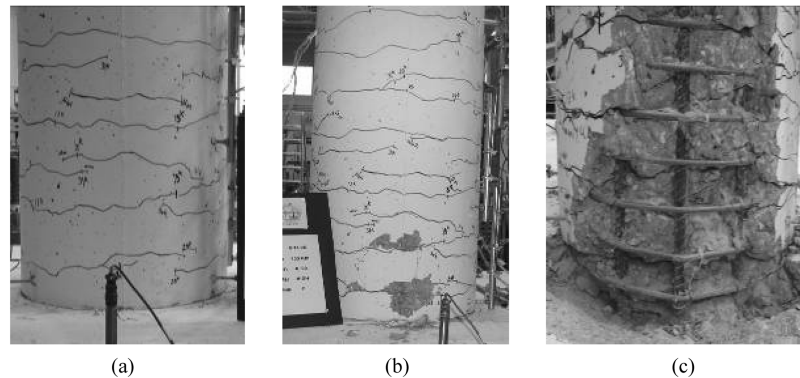


Fig. 5 Damage to column under bending shear at (a) first yielding of longitudinal bar, (b) peak lateral load, and (c) overall failure

18.0). The flexural hysteresis is shown in Fig. 4.

The flexural resistance was maintained at more or less constant levels between displacement of 110 mm and 460 mm, with nearly constant flexural moment strength of 850 kN-m. During the last cycle of loading, a longitudinal bar started buckling while unloading. The yielding zone of the longitudinal bars was about 610 mm from the base of the column. Longitudinal bars on both sides A and C both reached the yield strain at the predicted ductility level of one. The spirals remained elastic up to a ductility level of 6.0, after which they yielded. Soon after cracking and spalling at the location of the spiral gages, the spiral gages were damaged and data could no longer be collected. A typical progression of damage under bending shear is shown in Fig. 5.

### 3.2 Columns under cyclic pure torsion

In practice, pure torsion is rarely present in structural members; torsion usually occurs only in combination with other actions. However, understanding the behavior of members subjected to pure torsion is necessary for the analysis of a structural member under combined loading. Few studies have reported on the behavior of circular RC sections under pure torsion. Hindi *et al.* (2005) pioneered the use of two cross spirals to enhance the strength and ductility. The torsional strength of a member depends mainly on the amount of transverse and longitudinal reinforcement, the sectional dimensions, and the concrete strength. In post-peak behavior, the dowel action of longitudinal bars has also been reported to increase load resistance significantly at higher cycles of loading (Belarbi *et al.* 2008b).

Under pure torsional loading, significant diagonal cracks started developing near mid-height on the column at lower levels of ductility up to 3.0. The cracks propagated when the applied torsion was increased. As the test progressed, the diagonal cracks continued to form at an inclination and in a spiral form. Soon after cracking, the spirals yielded in the subsequent loading cycle, indicating that the spiral reinforcement ratio of 0.73% is the approximate minimum for a torsional design. A spiral reinforcement ratio of 1% is a more practical value in the design of bridge columns in the USA. To offset the cracking from the yielding level, the spiral reinforcement ratio was increased to 1.32% and again tested under pure torsion. The angle of diagonal cracks was about 39 to 42 degrees relative to the cross section plane of the column. The damage pattern of columns under pure torsion was significantly different from that of columns under bending combined with shear.

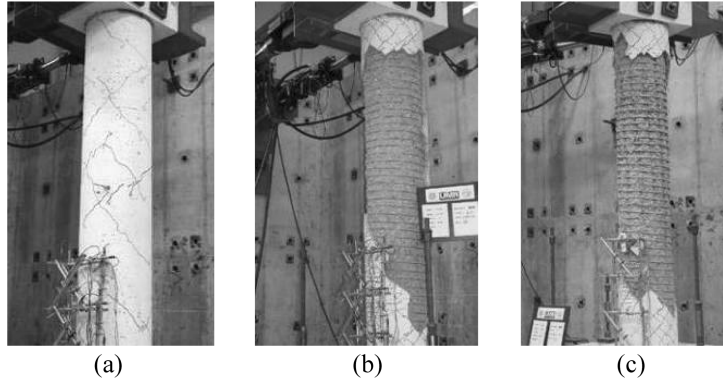


Fig. 6 Damage of column under pure torsion at (a) first yielding of spiral, (b) peak torsional moment, and (c) overall failure

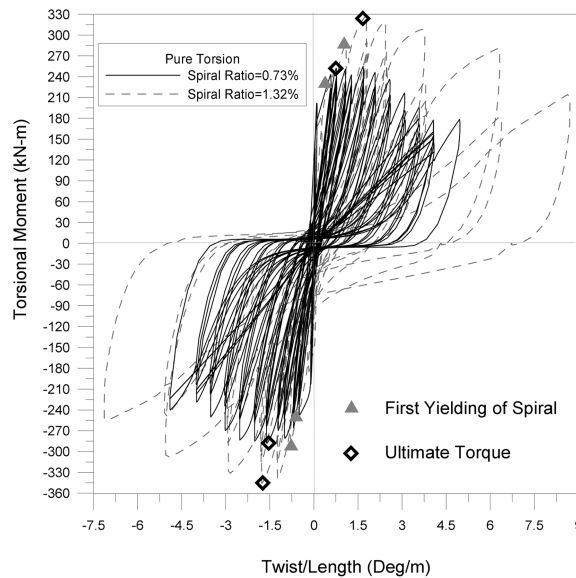


Fig. 7 Torsional hysteresis under pure torsion with various spiral reinforcement ratios

Typical damage to columns under pure torsion is shown in Fig. 6. The spalling occurred near the top of the column at the completion of the test.

The torsional moment versus twist hysteresis curves of specimens with spiral reinforcement ratios of 0.73% and 1.32% are compared in Fig. 7. These curves are approximately linear up to the point of cracking; thereafter, they become nonlinear with a drop in torsional stiffness. The post-cracking stiffness decreased proportionally with an increase in the cycles of loading until the effect of dowel action became apparent with a spiral reinforcement ratio of 0.73%. The column with a spiral reinforcement ratio of 1.32% had greater post-cracking stiffness and strength. The yielding strength increased up to 20% and the ultimate strength by 30% due to an increase in the spiral reinforcement ratio from 0.73% to 1.32%. The locking and unlocking effect of the spirals was also observed in both the negative and positive loading cycles. During the positive cycles of twisting, the spirals were unlocked, which contributed to significant spalling and reduced the confinement effect on the

concrete core. On the other hand, during the negative cycles of loading, the spirals were locked and contributed more to the confinement of concrete core. This effect is reflected in the asymmetry of the observed hysteresis loop at higher levels of loading. At higher cycles of loading, the load resistance in the negative cycles was higher than in the positive cycles of loading due to the added confinement generated by the locking effect of the spirals.

### 3.3 Columns under cyclic combined bending and torsion

Four columns were tested under combined bending and torsion by maintaining T/M ratios of 0.2 and 0.4 at two different spiral reinforcement ratios of 0.73% and 1.32%. The test results from columns under bending shear and pure torsion were used as the benchmarks for analyzing the behavior of specimens under combined bending-shear and torsion. In all the columns tested under combined bending and torsion, flexural cracks first appeared near the bottom of the column. With increasing cycles of loading and higher T/M ratios, the angle of the cracks became more inclined at increasing heights above the top of the footing. In all columns, side A of the column exhibited less damage than side C largely because that side A always experienced more shear stresses. These additional stresses were due to the additive components of stresses caused by shear and torsion; and they were greater than stresses in side C where torsional shear stresses were subtracted from shear stresses.

In general, three failure modes are possible under combined bending, shear, and torsion for a concrete member reinforced with longitudinal and transverse reinforcement: (1) completely under-reinforced for both low reinforcement directions (longitudinal and transverse steel yield) before concrete failure, (2) partially over-reinforced in terms of one reinforcement direction (only longitudinal steel yields or only transverse reinforcement yields depending on the relative amount of reinforcement in each direction), and (3) completely over-reinforced for both reinforcement directions (concrete compression failure before steel yields). The typical progression of damage under combined bending and torsion is shown in Fig. 8. The flexural hysteresis and torsional hysteresis of the column with a spiral reinforcement ratio of 0.73% and 1.32% and tested at a T/M ratio of 0.2 are compared in Fig. 9. The behavior of the specimen was dominated by both flexure and torsion. The failure of the specimen was by both flexural and torsional stiffness and strength degradation. Fig. 10 shows the flexural hysteresis and torsional hysteresis of the column with a spiral reinforcement ratio of 0.73% and 1.32% and tested at a T/M ratio of 0.4. The behavior of the specimen was dominated by

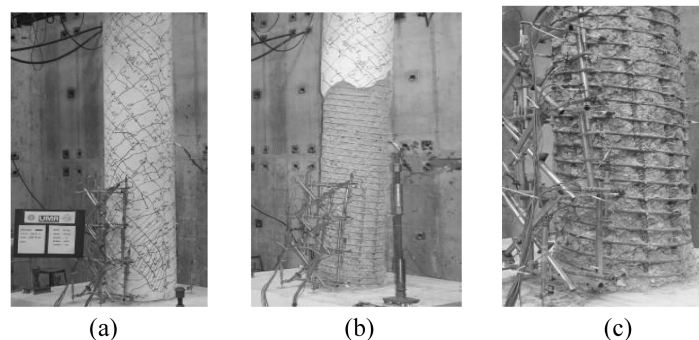


Fig. 8 Typical progression of damage under combined bending and torsion moments at (a) first yielding of longitudinal reinforcement (b) peak torsional moment and (c) overall failure

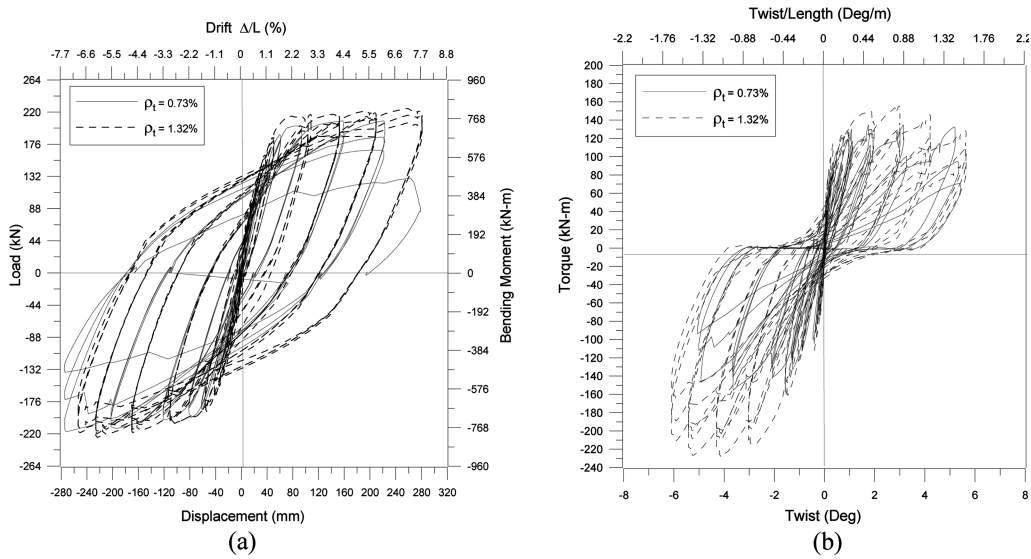


Fig. 9 Comparison of hysteresis behavior of T/M (0.2)-H/D (6) (a) flexural hysteresis and (b) torsional hysteresis

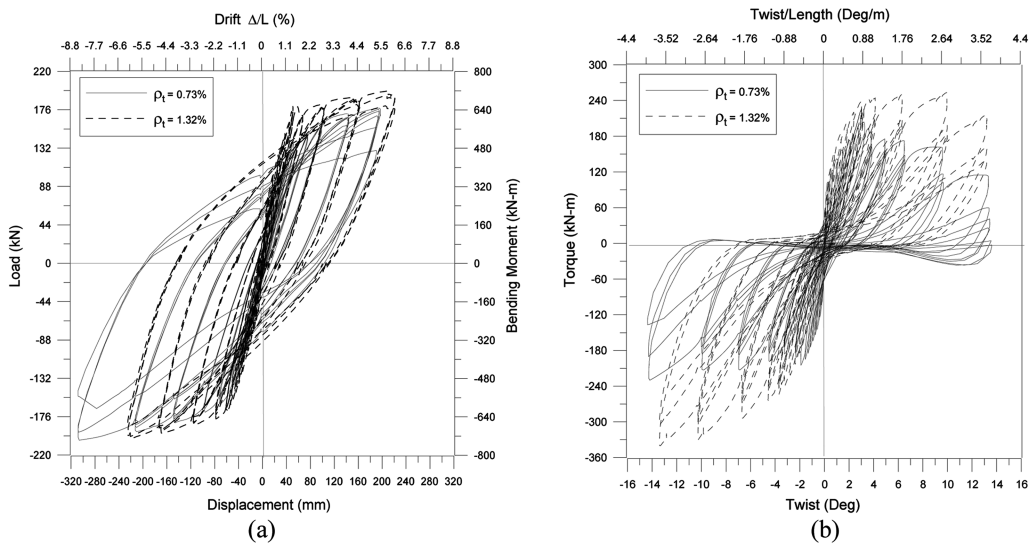


Fig. 10 Comparison of hysteresis behavior of T/M (0.4)-H/D (6) (a) flexural hysteresis and (b) torsional hysteresis

torsion. The flexural strength and stiffness of the specimen did not degrade before the failure by torsion. The asymmetric behavior of the hysteresis curve under both flexure and torsion revealed a significant difference due to the locking and unlocking. The lateral load displacement curves under combined loading are compared in Fig. 11(a). The torsional moment versus twist curves are compared in Fig. 11(b). These curves are due to the effect of combined loading, and torsional strength reduced with decreasing T/M ratio and bending strength reduced with increasing T/M ratio. The asymmetric nature of the torsional envelopes is due to the locking and unlocking

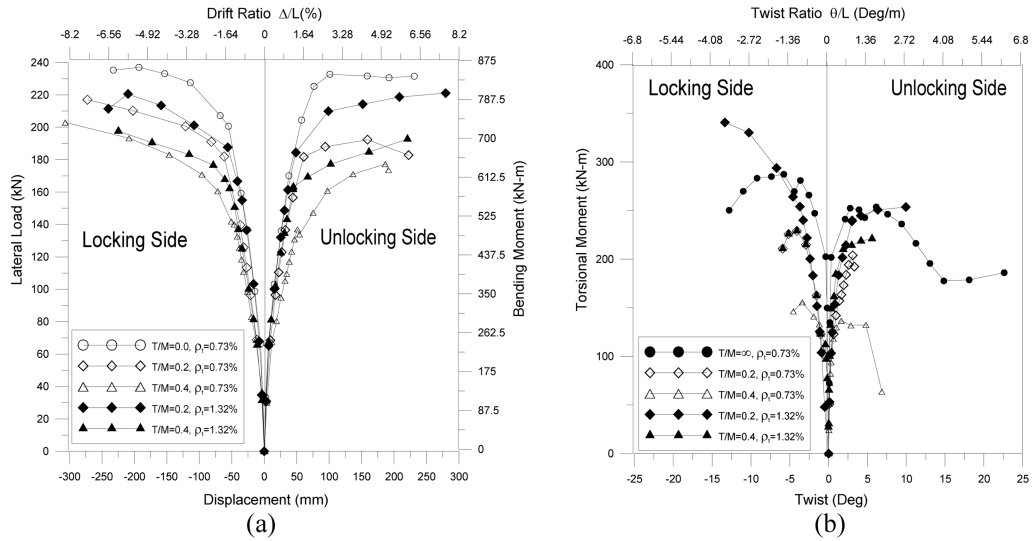


Fig. 11 Comparison of (a) lateral load displacement curves and (b) torsional moment-twist curves under combined bending and torsion moments

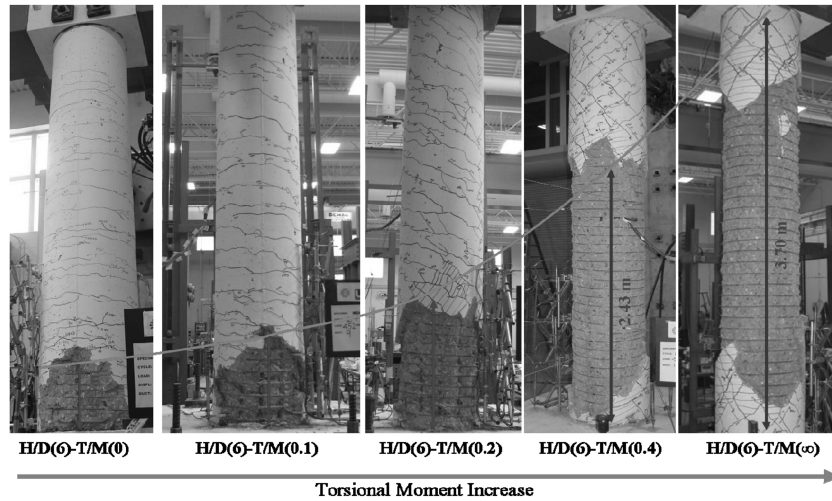


Fig. 12 Effect of combined loading on the damage length distribution

effect of the spirals. Due to the effect of combined loading, the post-cracking torsional stiffness degraded faster than that observed under pure torsion. Torsional strength, bending strength, and deformational capacity also improved significantly with an increase in the spiral reinforcement ratio.

The components of shear stresses from bending and torsion are additive, resulting in more damage and less load resistance. Thus, the asymmetric nature of the flexural envelopes under combined bending and torsion was due to the fact that one face was subjected to higher shearing stresses. The interaction of torsion and bending moments is shown in Fig. 12. The loading in the T/M ratio could not be maintained at a constant rate after the column reached its torsional strength. For the test column with a T/M ratio of 0.4, spalling and core degradation occurred through a height of 915 mm from the top of the foundation. For the column tested under bending and shear, the yielding zone of

the longitudinal bars and spalled region extended through a height of 610 mm from the base of the column for the column. The extent of this area shows that the flexural plastic hinge location changed due to torsion. However, the specific location of the plastic hinge depended on the applied T/M ratio. With increasing T/M ratio, the location of plastic hinge tends to increase from the bottom of the column to the middle height.

Bending moment curvature analyses are widely used as the basis for assessing the nonlinear force displacement response of an RC member subjected to inelastic deformation demands under seismic loads. The presence of torsion changes the damage location in a column, which changes the behavior under combined loading. The existing models were used to calculate the plastic hinge length. However, they were not accurate in predicting the plastic hinge length due to the effect of torsion. Methods for estimation of plastic hinge lengths proposed by Priestley *et al.* (1996) are not accurate in the presence of torsional loading since they do not yield practical results. Strain gage

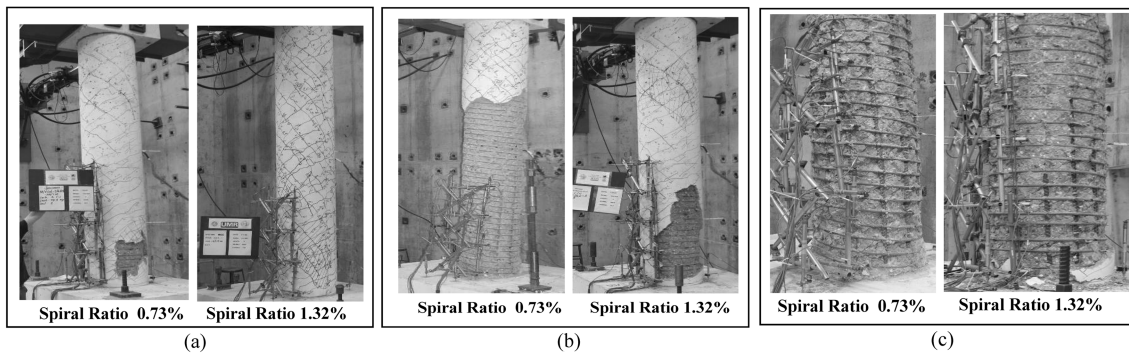


Fig. 13 Effect of spiral reinforcement ratio on failure modes under combined bending and torsion ( $T/M=0.4$ ) at (a) first yielding of spiral, (b) peak torsional moment, and (c) overall failure

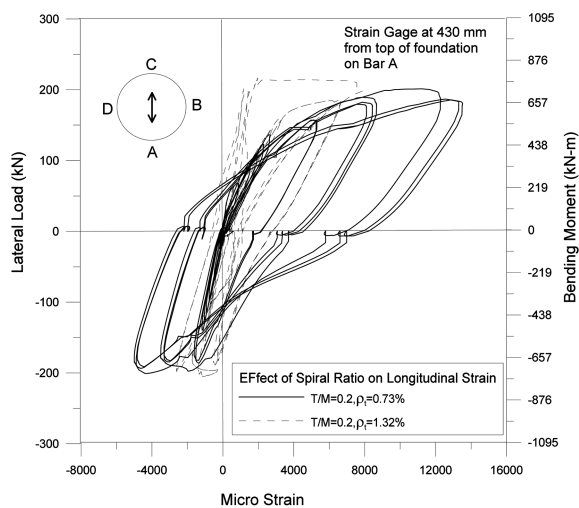


Fig. 14 Effect of spiral reinforcement ratio on longitudinal strain distribution under combined bending and torsion moments at  $T/M (0.2)$

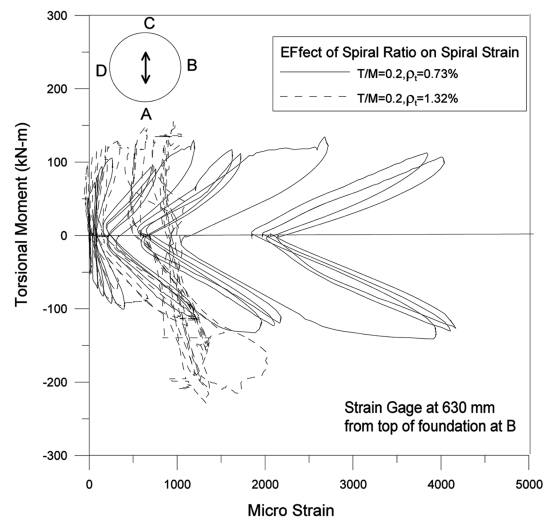


Fig. 15 Effect of spiral reinforcement ratio on spiral strain distribution under combined bending and torsion moments at  $T/M (0.2)$

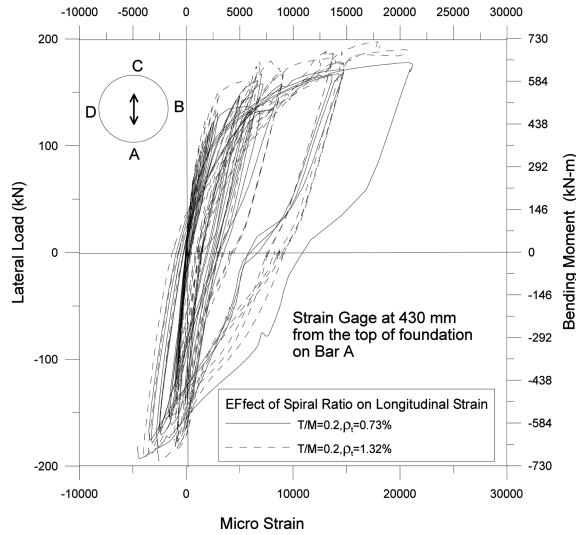


Fig. 16 Effect of spiral reinforcement ratio on longitudinal strain distribution under combined bending and torsion moments at T/M (0.4)

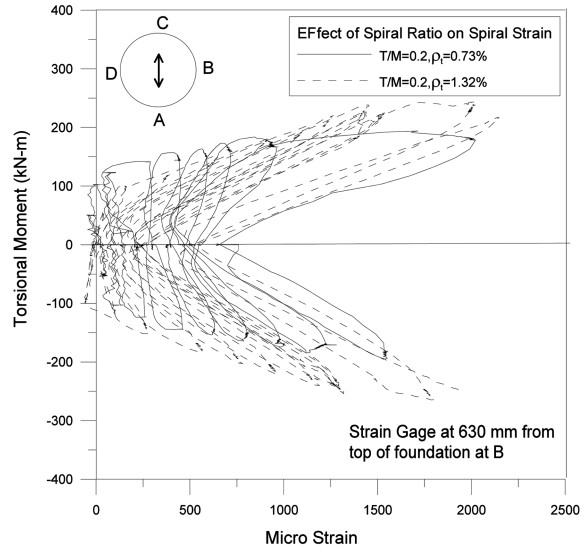


Fig. 17 Effect of spiral reinforcement ratio on spiral strain distribution under combined bending and torsion moments at T/M (0.4)

readings from test specimens were used to calculate the plastic hinge length using the yield zone of reinforcements under tension. Test results show that with increase in torsion to bending moment ratio, there is an increase in length of damage zone along with change in its location (Fig. 12). In all columns under combined bending and torsion moments, failure started due to severe combinations of shear and flexural cracks leading to progressive spalling of the cover concrete. The columns under combined loading finally failed due to significant core degradation followed by buckling of longitudinal bars on side C.

The effect of an increasing spiral reinforcement ratio on the progression of failure under combined loading is shown in Fig. 13. This increase limited the damage at spiral yielding and at ultimate torsional moment when compared to the column with a lower spiral reinforcement ratio. The effect of an increased spiral reinforcement ratio on longitudinal and spiral strain distribution for test columns with T/M=0.2 is shown in Figs. 14 and 15. The same effect on test column with T/M=0.4 is shown in Figs. 16 and 17. Although an increase in the spiral reinforcement ratio reduced longitudinal strain only marginally, spiral strains reduced considerably in test columns with both T/M=0.2 and T/M=0.4 at the same load level. This reduction shows that an increase in the spiral reinforcement ratio limits the torsional damage by increasing the torsional strength and stiffness under combined bending and torsion.

### 3.4 Effect of spiral reinforcement ratio on torsion-bending moments interaction diagram

Torsion-bending moment curves for the columns tested under combined bending and torsional moments are shown in Fig. 18. These curves indicate that the test columns reached their torsional capacity prior to reaching their flexural capacity. However, the longitudinal reinforcement yielded before the spiral reinforcement yielded. Hence, the failure sequence in all test columns was flexural cracking, followed by shear cracking, longitudinal reinforcement yielding, spalling, and spiral yielding.

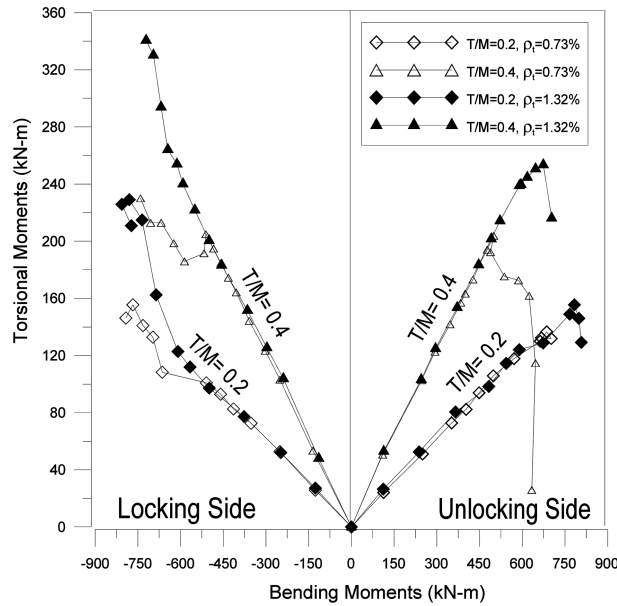


Fig. 18 Comparison of torsion-bending moments curves for various combined loading ratios

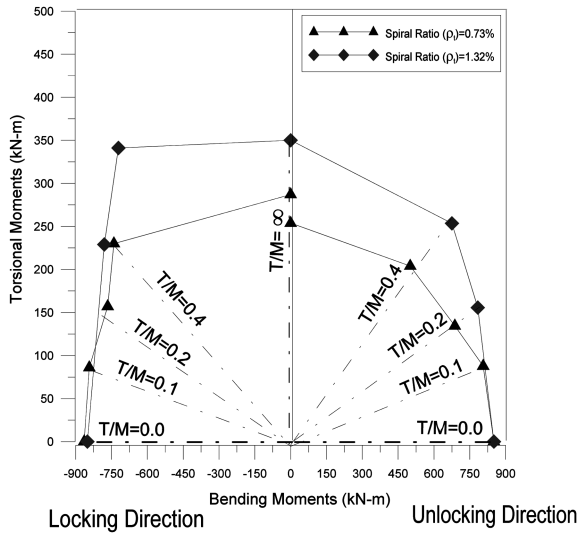


Fig. 19 Torsion-bending interaction diagram at peak torque

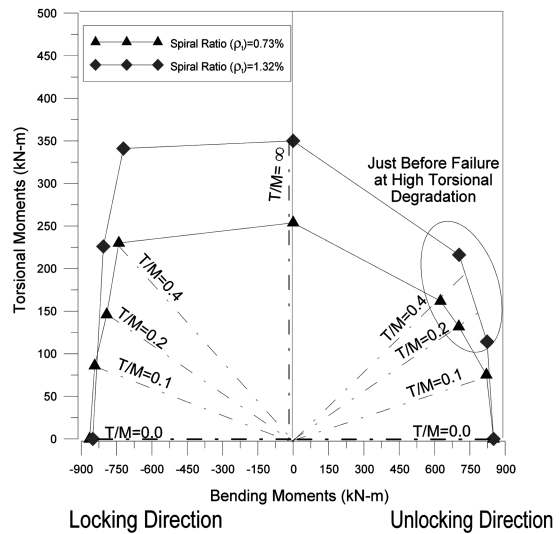


Fig. 20 Torsion-bending moments interaction diagram at peak shear

Overall failure occurred finally with buckling of the longitudinal bars immediately after significant core degradation. Yielding of longitudinal and spiral reinforcement occurred at roughly same time for the test column with a spiral reinforcement ratio of 0.73%. With an increase in the spiral reinforcement ratio, torsional and bending strengths improved significantly. More importantly, significant twist ductility was achieved in torsional moment-twist behavior.

For all test columns, torsion-bending moment interaction diagrams were created for peak torsional moment (Fig. 19) and peak shear (Fig. 20). The T/M ratio was maintained close to the desired

loading ratio in all columns until peak torsional moment was attained in the unlocking direction. Soon after peak torsional strength, the desired loading ratio could not be maintained because torsional stiffness degraded much faster in both the unlocking and locking directions. However, bending strength degraded faster than torsional strength in the locking direction for the columns with a spiral reinforcement ratio of 1.32%, hence, the load ratio could not be maintained to complete the test. When RC columns are subjected to torsional loading along with pure bending, the flexural strength and stiffness of column members decreases significantly. More importantly, the ductility and energy dissipation capacity under flexure are also reduced significantly. Plastic hinge forms at the maximum moment location under flexure. However, the presence of torsion significantly changes the damage distribution under combined loading. Hence, the design detailing should also change accordingly in the columns where torsional moments are anticipated in design.

#### 4. Finite element (FE) analysis

A nonlinear finite element (FE) analysis was performed and compared with the test results using the commercial program DIANA (Displacement ANALyzer). All columns tested under combined loading were analyzed through three-dimensional FE models with the corresponding loading protocol used in the test. The overall geometry of the FE model is the same as that of the test column, and some assumptions were made for test set-up. Fig. 21 provides a detailed description of the FE model. An eight-node isoparametric solid brick element (HX24L in DIANA) was chosen to model the concrete and loading blocks. Based on the rotating crack behavior, the material behavior of the concrete elements followed an orthotropic smeared crack model, parallel to the principal strain directions. The concrete material model follows that proposed by Thorenfeldt *et al.* (1987) with the consideration of softening and confinement effects for concrete under compression. The softening effect is considered in the FE model using the softening model proposed by Vecchio and Collins (1993) and the confinement effect is considered in the model proposed by Selby and Vecchio (1993). Fig. 22 shows the compressive stress-strain curves with respect to each lateral strain effect.

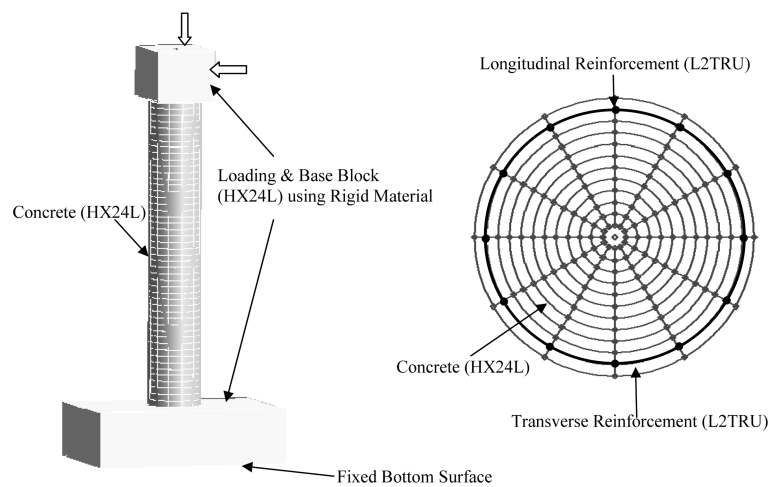


Fig. 21 Finite element model of columns

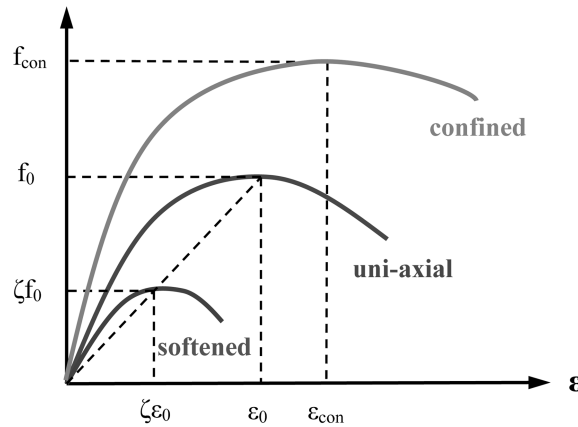


Fig. 22 Compressive stress-strain curves for concrete

In cracked concrete, large tensile strains perpendicular to the principal compressive direction reduce the concrete compressive strength (Mo and Hsu 1985). Consequently, compressive strength is not only a function of the uni-axial compressive strain,  $\varepsilon_1$ , but also a function of the lateral strains governing the tensile damage in the lateral directions,  $\varepsilon_2$  and  $\varepsilon_3$ . However, the modified compression field theory (MCFT) proposed by Vecchio and Collins (1993) used in DIANA is derived and calibrated from two-dimensional problems. To adapt the MCFT to a three-dimensional problem, DIANA assumes two lateral strains perpendicular to the principal compressive direction as an average lateral strain given by  $\varepsilon_{lat} = \sqrt{\varepsilon_2^2 + \varepsilon_3^2}$ . A rigid linear elastic material model is applied to the loading and base blocks to minimize the negative influence of both blocks on the behavior of a column. The reinforcing steels were modeled as embedded bar elements specialized by DIANA and assumed to be elasto-plastic considering the strain hardening effect.

A regular Newton-Raphson method was used for the iteration method with a maximum of twenty iterations. The number of iterations is determined based on the preliminary analysis which showed convergence problems due to the post-peak decay in strength and stiffness of concrete. As a convergence criterion, the norms of the force and displacement fields were applied with the values of 0.045 N and 0.254 mm, respectively. It means that besides stopping the iteration in case of convergence, the iteration process is also stopped if a specified maximum number of iterations have been reached or if it led to divergence. The detection of divergence is based on the same norms as that of convergence.

## 5. Results and discussion of FE analysis

### 5.1 Overall behavior

Although all analytical results show somewhat stiffer behavior than experimental results due to the smeared crack model adopted in FE analysis, the FE model can adequately predict the overall behavior of test columns except for the column with a low spiral reinforcement ratio of 0.73% subjected to a high T/M ratio of 0.4. The behavior of specimens tested at lower T/M ratios was dominated by flexural behavior; that is, the flexural displacement ductility of these specimens was

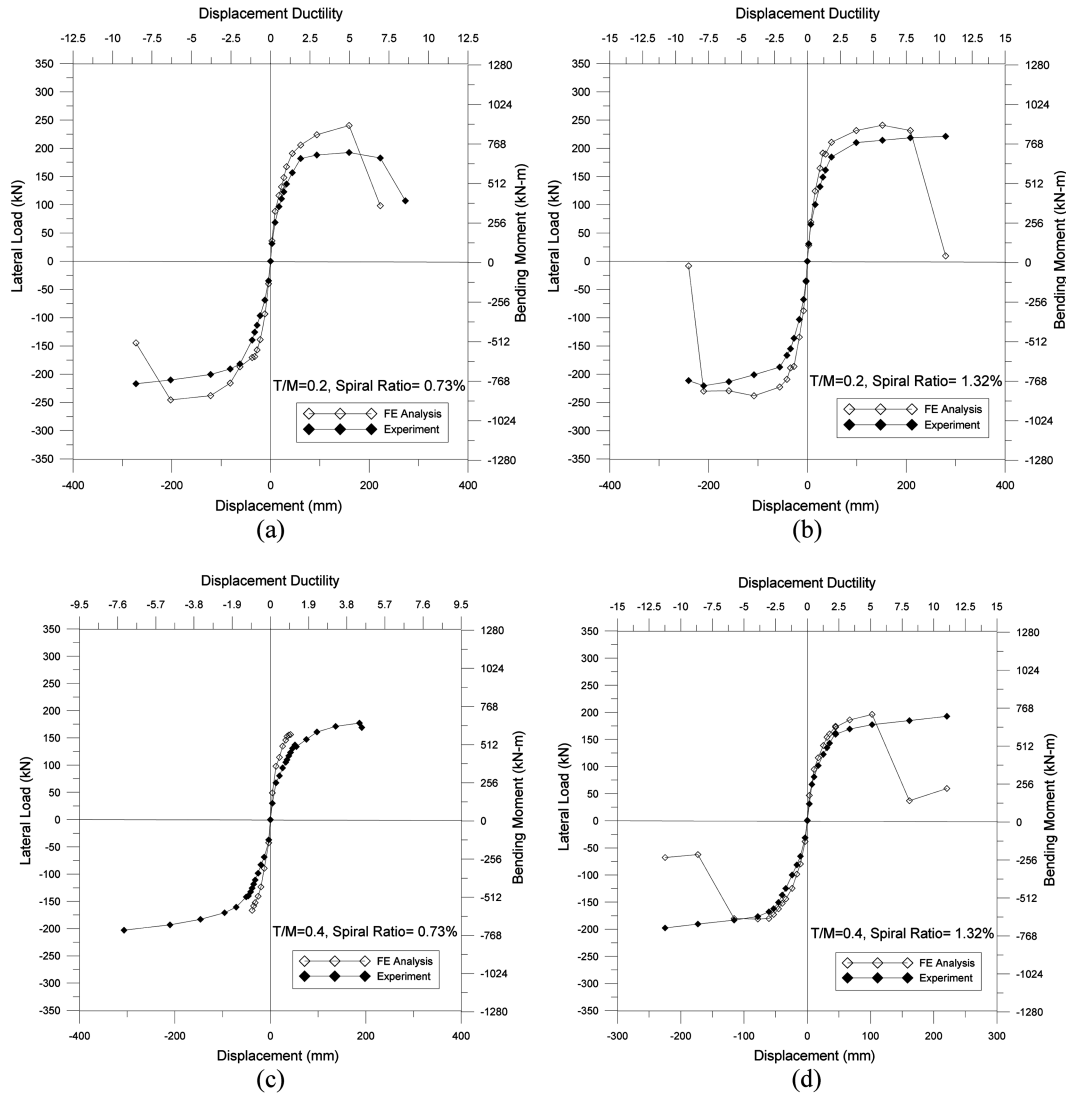


Fig. 23 Comparisons of lateral load-displacement curves under combined bending and torsion moments

higher than that of specimens tested at higher  $T/M$  ratios, as shown in Fig. 23.

In the case of columns tested at higher  $T/M$  ratios, torsional behavior was predominant. Therefore, the torsional rotation ductility was higher than the flexural displacement ductility in these columns as shown in Fig. 24. As a result, flexural displacement ductility decreased with an increase in the  $T/M$  ratio, indicating that applied torsional moment has an adverse effect on flexural capacity as shown in the experimental results. Increasing the spiral reinforcement ratio is very effective in improving both torsional moment capacity and bending moment capacity because it suppresses the torsional effect that causes sudden brittle failure due to excessive shear stresses in the weak region. Thus, a proper spiral reinforcement ratio can ensure not only an increase in the torsional moment capacity but also in flexural capacity through confinement.

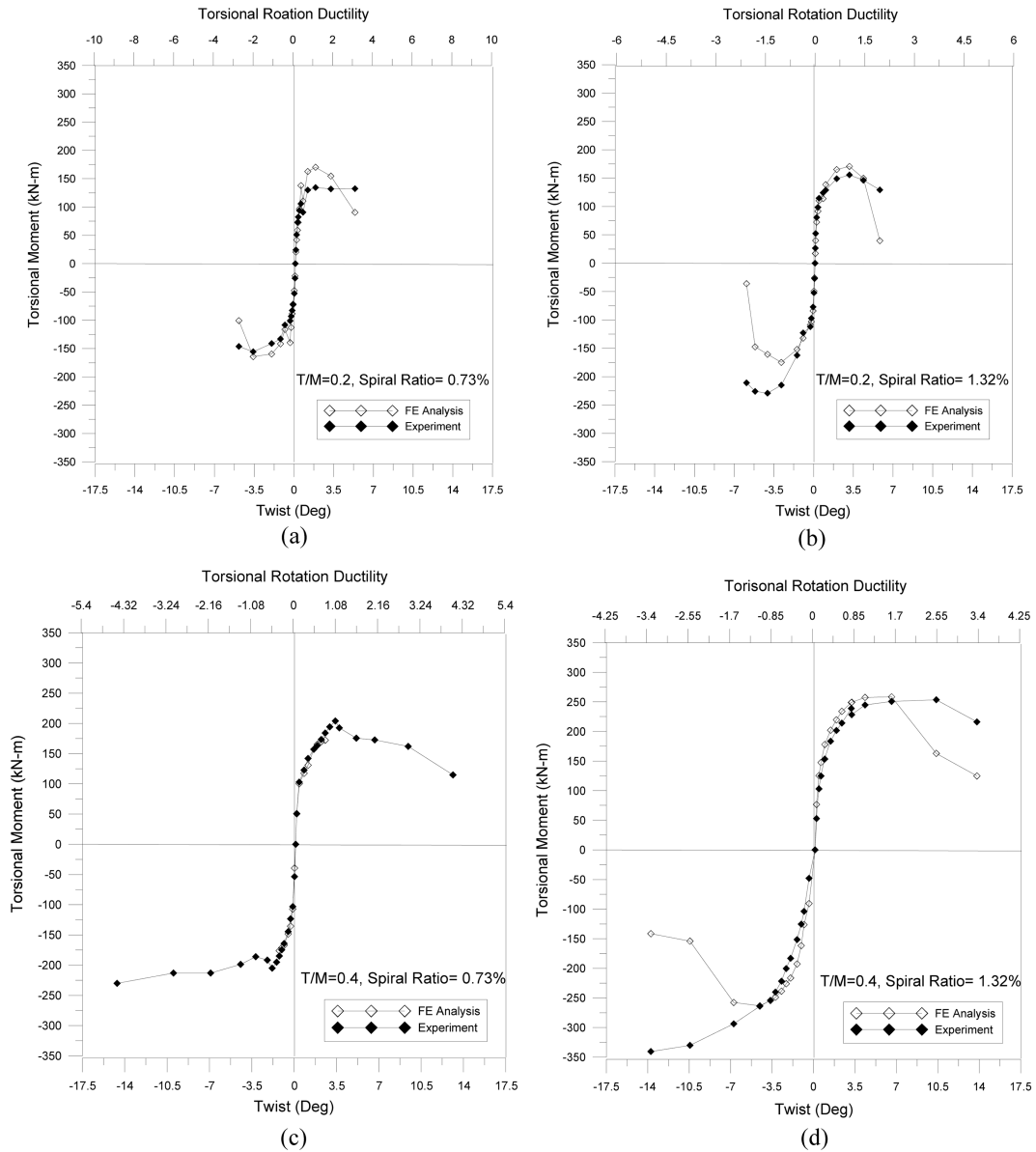


Fig. 24 Comparison of torsional moment-twist curves under combined bending and torsion moments

### 5.2 von Mises stress variations

von Mises stress variations on the outer surface and mid-section are shown in three- and two-dimensional layouts in Fig. 25, to illustrate in detail the effect of an increase in spiral reinforcement. Although the spalling effect cannot be simulated in a FE model, failure modes and damage levels in a column can be sufficiently explained by these results. Damage on the outer surface was significantly decreased along the whole length of the column with an increase in the spiral reinforcement ratio. Thus, increased spiral reinforcement ratio can provide more torsional capacity, ultimately

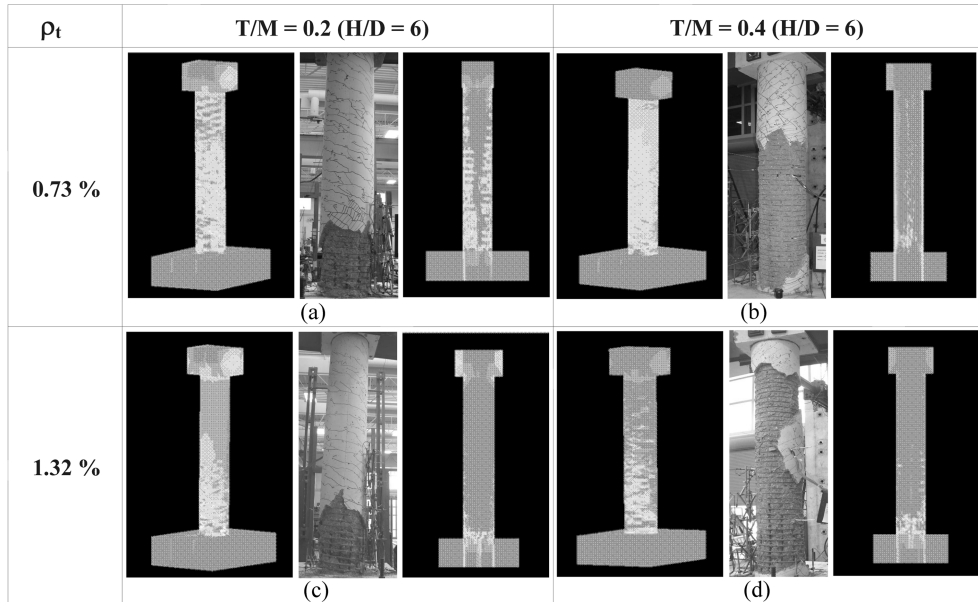


Fig. 25 von Mises stress variation at overall failure under combined bending and torsion moments

resulting in the change of the failure mode from torsional dominant to flexural dominant. As shown in the Fig. 25, severe damage occurred in the lower part of the columns with spiral reinforcement ratio of 1.32%, regardless of T/M ratios.

Besides the effect of the spiral reinforcement ratio, several stress variations were apparent with respect to various T/M ratios. When the T/M ratio increased, von Mises stresses were well distributed in the outer surface along the length of the column due to additional shear stresses from torsion and shear. The opposite occurred with a relatively lower T/M ratio. As shown in Fig. 25, von Mises stresses tend to spread into the core area. From a design point of view, columns shall be designed for combined loading leading to flexure failure, because this failure mode is predictable according to well established theory. Thus, the failure modes of columns under combined loading can be changed by the proper detailing of spiral reinforcement ratios.

## 6. Summary and concluding remarks

This paper presents the results of tests on columns under bending and shear, pure torsion, and combined bending, shear and torsion, and it discusses the effects of increasing the spiral reinforcement ratio on strength, stiffness, and damage characteristics. Both the test results and the FE analysis suggest the following conclusions:

- The degradation in strength of a column under pure torsion is contained by increasing the spiral reinforcement ratio. Such an increase improves the torsional strength and rotational ductility by increasing deformational capacity after yielding.
- An increase in the spiral reinforcement ratio results in more confinement and thus reduces the degradation of bending and torsional strength under combined bending moments and torsion.
- An increase in the spiral reinforcement ratio limits the damage corresponding to spiral yielding

and peak torque of column under combined bending and torsional moment when compared to the one with a lower spiral reinforcement ratio.

- By including the softening and confinement effect, FE models can accurately predict the behavior of columns under combined bending and torsion in most cases. In this study, the column tested at a high T/M ratio of 0.4 and a spiral reinforcement ratio of 0.73% was an exception; this column was considered lightly reinforced for the amount of torsion applied.

## Acknowledgements

This study was funded by NSF-NEESR under Grant No. NEESR-SG: 530737, the National University Transportation Center, and the Intelligent Systems Center of Missouri S&T. Their financial support is gratefully acknowledged.

## References

- Belarbi, A., Suriya Prakash, S. and Silva, P. (2008a), "Flexure-shear-torsion Interaction of RC bridge columns", *Proc. of the Concrete Bridge Conference*, St. Louis, USA, Paper No. 6.
- Belarbi, A., Suriya Prakash, S. and Ayoub, A. (2008b), "An experimental study on behavior of RC bridge columns under combined cyclic bending and torsion", *Proc. of the Concrete Bridge Conference*, St. Louis, USA, Paper No. 5.
- Elwood, K.J. and Moehle, J.P. (2005), "Drift capacity of reinforced concrete columns with light transverse reinforcement", *Earthq. Spectra*, **21**(1), 71-89.
- Hindi, R., Al-Qattawi, M. and Elsharief, A. (2005), "Influence of different confinement patterns on the axial behavior of R/C columns", *Structures Congress*, ASCE, New York, USA.
- Hsu, H.L. and Wang, C.L. (2000), "Flexural-torsional behavior of steel reinforced concrete members subjected to repeated loading", *Earthq. Eng. Struct. Dyn.*, **29**, 667-682.
- Lehman, D.E., Calderone, A.J. and Moehle, J.P. (1998), "Behavior and design of slender columns subjected to lateral loading", *Proc. of the Sixth U.S. National Conference on Earthquake Engineering*, EERI, Oakland, California, May 31-June 4, Paper No. 87.
- Mo, Y.L. and Hsu, T.T.C. (1985), "Softening of concrete in torsional members- design recommendations", *ACI Struct. J.*, **82**(37), 443-452.
- Mostafaei, H. and Kabeyasawa, T. (2007), "Axial-shear-flexure interaction approach for reinforced concrete columns", *ACI Struct. J.*, **104**(2), 218-226.
- Otsuka, H., Takeshita, E., Yabuki, W., Wang, Y., Yoshimura, T. and Tsunomoto, M. (2004), "Study on the seismic performance of reinforced concrete columns subjected to torsional moment, bending moment and axial force", *Proc. of the 13<sup>th</sup> World Conf. on Earthquake Engineering*, Vancouver, Canada, Paper No. 393.
- Park, Y.J. and Ang, A.H.S. (1985), "Mechanistic seismic damage model for reinforced concrete", *J. Struct. Eng.*, ASCE, **111**(4), 722-739.
- Priestly, M.J.N. and Benzoni, G. (1996), "Seismic performance of circular columns with low longitudinal reinforcement ratios", *ACI Struct. J.*, **93**(4), 474-485.
- Priestly, M.J.N., Seible, F. and Calvi, G.M. (1996), *Seismic Design and Retrofit of Bridges*, John Wiley and Sons, Inc., New York.
- Selby, R.G. and Vecchio, F.J. (1993), "Three-dimensional constitutive relations for reinforced concrete", University of Toronto, Toronto, Canada. Tech. Report No. 93-02.
- Suriya Prakash, S., Belarbi, A. and Ayoub, A. (2008), "Cyclic behavior of RC bridge columns under combined loadings including torsion", *Sixth Seismic National Conference on Highways and Bridges*, July 27-30, Charleston, South Carolina, USA.

- Suriya Prakash, S. and Belarbi, A. (2009), "Towards damage-based design approach for RC bridge columns under combined loadings using damage index models", *J. Earthq. Eng.* (in press).
- Thorenfeldt, E., Tomaszewicz, A. and Jensen, J.J. (1987), "Mechanical properties of high-strength concrete and applications in design", *Proc. of Symp. Utilization of High-Strength Concrete*, Tapir, Trondheim, Stavanger, Norway, 149-159.
- Tirasit, P. and Kawashima, K. (2007), "Seismic performance of square reinforced concrete columns under combined cyclic flexural and torsional loadings", *J. Earthq. Eng.*, **11**, 425-452.
- Tirasit, P. and Kawashima, K. (2008), "Effect of nonlinear torsion on the performance of skewed bridge piers", *J. Earthq. Eng.*, **12**, 980-998.
- Vecchio, F.J. and Collins, M.P. (1993), "Compression response of cracked reinforced concrete", *J. Struct. Eng.*, ASCE, **119**(12), 3590-3610.